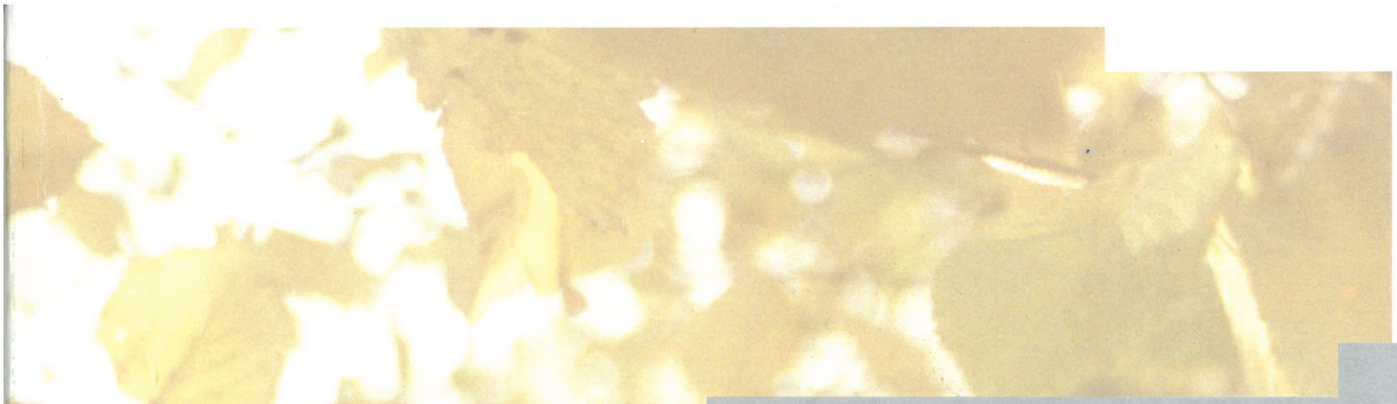

Laboratoire d'Informatique
pour la Mécanique
et les Sciences de l'Ingénieur

NOTES ET DOCUMENTS LIMSI N° : 95 - 06
Février 1995

Approximation inconditionnellement stable par éléments finis et méthode de projection pour les équations de Navier–Stokes instationnaires

Jean-Luc GUERMOND et Luigi QUARTAPELLE

limsi
Centre National de la Recherche Scientifique
LIMSI-CNRS - BP 133, F-91403 ORSAY Cedex (France)

UNCONDITIONALLY STABLE PROJECTION METHODS FOR FINITE ELEMENT SOLUTION OF THE UNSTEADY NAVIER–STOKES EQUATIONS

J.-L. GUERMOND* AND L. QUARTAPELLE†

Abstract. This paper describes the main features of a fractional-step projection method and its finite-element implementation using unstructured triangular meshes to compute incompressible viscous flows in domains of arbitrary shape and under quite general boundary conditions. The basic idea in the derivation of this method is that the appropriate functional setting for projection methods must accommodate two different spaces for representing the two velocity fields calculated in the viscous and incompressible half steps of the method. Such a theoretical distinction leads to a finite element projection method with a Poisson equation for the pressure increment free from any boundary condition difficulty and to a very practical implementation of the method with only the intermediate velocity appearing in the numerical algorithm. An unconditionally stable semi-implicit approximation of the nonlinear convection term is used to eliminate any stability restriction on the time step. The numerical solutions of two test problems in two dimensions calculated by the proposed method compare quite satisfactorily with the reference solutions.

Key words. Projection method, Fractional-step method, Incompressible Navier–Stokes equations, Finite elements.

AMS(MOS) subject classifications. 35A40, 35Q10, 65J15

1. Introduction.

The fractional-step projection method of Chorin [6, 7] and Temam [28] (see also [27] and [23]) is the most frequently employed technique for the numerical solution of the primitive variable Navier–Stokes equations. This method is based on a rather peculiar time-discretization of the equations governing viscous incompressible flows, in which the viscosity and the incompressibility of the fluid are dealt within two separate steps. Such time-stepping algorithm can be combined with any kind of spatial discretization technique, *viz.*, finite differences (see *e.g.* Bell *et al.* [2]), finite elements (Donea *et al.* [9], Gresho and Chan [14]), or spectral approximations (Ku *et al.* [19]).

An important, although almost never analyzed, feature of fractional-step projection methods is the structural difference existing between the equations of the viscous step and those of the incompressible phase of the calculation. In fact the first half-step constitutes an elliptic boundary value problem for an intermediate velocity unknown accounting for the viscous diffusion and convection mechanisms, whereas the second half-step represents an essentially inviscid problem which determines the end-of-step divergence-free velocity field together with a suitable approximation to the pressure distribution. In particular, boundary conditions of a different kind have to be imposed on the velocity fields which are calculated in each of the two half-steps.

* Laboratoire d'Informatique pour la Mécanique et les Sciences de l'Ingénieur, CNRS, BP 133, 91403, Orsay, France (guermond@limsi.fr).

† Dipartimento di Fisica, Politecnico di Milano, Piazza Leonardo da Vinci, 32, 20133 Milano, Italy.

In spite of that, most (if not all) actual implementations of the projection method assume implicitly one and the same discrete representation for the two aforementioned velocity fields. But the chosen approximation cannot afford the best representation of velocity simultaneously for both the viscous and inviscid phase of the method. For instance, finite difference spatial discretizations based on staggered grids, such as the celebrated MAC computational molecule, are appropriate for representing the equations of the inviscid projection step but not for the vector elliptic equation of the viscous step. Conversely, finite element discretizations using a continuous representation of the velocity variable by means of piecewise linear or multilinear polynomial interpolations are very suited for dealing with the viscous diffusion step but have a continuity degree higher than required by the equations of the inviscid step.

A functional analytical setting which properly accounts for the different character of the equations of the two half-steps has been proposed recently by the first author [15, 16]. The aim of this work is to describe the implementation of a finite-element fractional-step projection method which fully exploits the different mathematical structure of the equations for the two half-steps, as well as its consequences at the level of the spatially discretized equations. Insufficient consideration of this circumstance lies at the origin of the difficulties which the implementation of fractional-step projection methods is still encountering at present.

The content of the paper is organized as follows. In section 2 the unsteady Stokes problem supplemented by boundary conditions of a general kind is first formulated in differential form. A variational statement of the problem is then given, proving its equivalence with the original differential formulation and its well posedness. The abstract setting for the spatial discretization of the unsteady Stokes problem is finally introduced.

Section 3 describes an incremental version of the fractional-step time discretization algorithm for the Stokes problem and introduces the additional tools needed to have an abstract formulation of the spatially discrete equations of the two steps. Two possible numerical realizations of the equations enforcing incompressibility (the projection step) are considered, one regarding the projection step as a Darcy problem and the other as a Poisson problem for the pressure. Special attention is devoted to the boundary conditions which are imposed on the pressure in each of the two steps.

Section 4 addresses the full nonlinear problem of the incompressible Navier–Stokes equations. A convenient treatment for the nonlinear convection term is recalled and is shown to lead to a semi-implicit but unconditionally stable algorithm even in the presence of outflow boundaries.

Section 5 describes the spatial discretization by means of finite elements with linear interpolation of the unknown variables for the solution of flow problems in two dimensions. The numerical tools employed for generating unstructured Delaunay triangulations and for solving the finite element equations are indicated. The complete numerical procedure is then applied to two test problems, the driven cavity and the backward facing step, and the computed numerical solutions are compared with the benchmark solutions. The last section is devoted to some concluding remarks.

2. The unsteady Stokes problem.

2.1. Hypotheses and notations. Let Ω be an open connected bounded domain of $\mathbb{R}^d$ ($d = 2$ or 3 in practical applications) with a smooth boundary $\partial\Omega$; say $\partial\Omega$ is Lipschitz and Ω is locally on one side of its boundary. In the sequel, the set of real functions infinitely differentiable with compact support in Ω is denoted by $\mathrm{D}(\Omega)$. The set of distributions on Ω is denoted by $\mathrm{D}'(\Omega)$. As usual, $L^2(\Omega)$ denotes the space of real-valued functions, the squares of which are summable in Ω. We denote the inner product in $L^2(\Omega)$ by $(\cdot\,,\cdot)$ and its norm by $|\cdot|_0$. $H^m(\Omega)$, $m \geq 0$, is the set of distributions the successive derivatives of which, up to order m, can be identified with square summable functions. The space $H^m(\Omega)$, equipped with the norm $|u|_m^2 = (\sum_{|\alpha|=0}^m |D^\alpha u|_0^2)^{1/2}$, expressed in the multi-index notation, is a Hilbert space.

In order to introduce the fractional-step projection method and illustrate the ability of this technique to take into account a great variety of boundary conditions, we consider the following unsteady Stokes problem, hereafter referred to as $\mathcal{P}_0$, in which a unit kinematic viscosity has been assumed for simplicity. For a given body force f and velocity field u^* (both possibly dependent on time) and a given (divergence free) initial velocity field u_0, find a velocity field u and a pressure field p (with regularities yet to be clearly defined) so that at $t = 0$, $u = u_0$, and at all subsequent times

$$\mathcal{P}_0 \quad \begin{cases} \dfrac{\partial u}{\partial t} - \nabla^2 u + (u^* \cdot \nabla) u + \nabla p = f, \\ \nabla \cdot u = 0, \end{cases} \tag{2.1}$$

the velocity and the pressure being subject to the following boundary conditions:

$$\begin{aligned} u_{|\partial\Omega_1} &= 0; \\ u \cdot n_{|\partial\Omega_2} = 0, \qquad & (\alpha u + \nabla \times u) \times n_{|\partial\Omega_2} = 0; \\ u \times n_{|\partial\Omega_3} = 0, \qquad & p_{|\partial\Omega_3} = 0; \end{aligned} \tag{2.2}$$

where $\partial\Omega_1$, $\partial\Omega_2$, $\partial\Omega_3$ is a partition of $\partial\Omega$. The function α is defined on $\partial\Omega_2$ and is assumed to be suitably smooth. As shown below, these boundary conditions are closely related to the bilinear form $(\nabla\cdot u, \nabla\cdot v) + (\nabla\times u, \nabla\times v)$. Of course, other types of boundary conditions are possible; in particular if we associate with the Laplace operator the bilinear form $(\nabla u, \nabla v)$, we can enforce a series of natural boundary conditions associated to this form. All what is said in this paper can be readily adapted to this case. For sake of generality, we are considering boundary conditions different from purely Dirichlet conditions only for the velocity. Note that boundary conditions involving the tangential components of $\nabla\times u$ or u couple in general the Cartesian vector components of the velocity field when the boundaries $\partial\Omega_2$ and $\partial\Omega_3$ are curved or are flat but with an arbitrary orientation with respect to the Cartesian axes. There are however situations in which the Cartesian components of the velocity uncouple even

with boundary conditions different from the purely Dirichlet ones (*cf.* for instance the second problem of the numerical tests).

The vector field u^* is assumed to be smooth and divergence free. It defines a partition $(\partial\Omega_{in}, \partial\Omega_{out})$ of $\partial\Omega$ as follows:

$$\partial\Omega_{in} = \{x \in \partial\Omega,\ u^* \cdot n(x) < 0\}, \tag{2.3}$$

$$\partial\Omega_{out} = \{x \in \partial\Omega,\ u^* \cdot n(x) \geq 0\}. \tag{2.4}$$

We assume that $\partial\Omega_{in} \subset \partial\Omega_1$. Insofar as we are interested in the linear problem, these hypotheses are not necessary but simplify the presentation; they play instead an important role when the scheme is adapted to the Navier–Stokes equations (see further sections) for they yield unconditional stability (in some adequate norms yet to be specified).

2.2. The variational formulation. In order to formulate the unsteady Stokes problem in a variational form, we define the following Hilbert spaces:

$$X = \{v \in H^1(\Omega)^d,\ v_{|\partial\Omega_1} = 0,\ v \cdot n_{|\partial\Omega_2} = 0,\ v \times n_{|\partial\Omega_3} = 0\} \tag{2.5}$$

$$M = L^2(\Omega) \tag{2.6}$$

$$V = \{v \in X,\ \nabla\cdot v = 0\} \tag{2.7}$$

$$H = \{v \in L^2(\Omega)^d,\ \nabla\cdot v = 0,\ v \cdot n_{|\partial\Omega_1 \cup \partial\Omega_2} = 0\} \tag{2.8}$$

It can be shown that H is the completion of V in $L^2(\Omega)^d$. Denote by $H^1_{0,\partial\Omega_3}(\Omega)$ the space of scalar functions of $H^1(\Omega)$ the trace of which is zero on $\partial\Omega_3$. The importance of H is brought to light by the following orthogonal decomposition of $L^2(\Omega)^d$.

PROPOSITION 2.1. $L^2(\Omega)^d = H \oplus \nabla(H^1_{0,\partial\Omega_3}(\Omega))$.

Proof. For all f in $L^2(\Omega)^d$, denote by p the unique solution in $H^1_{0,\partial\Omega_3}(\Omega)$ of the following problem

$$\forall q \in H^1_{0,\partial\Omega_3}(\Omega), \qquad (\nabla p, \nabla q) = (f, q).$$

It is an easy matter to verify that $v = f - \nabla p$ is in H. □

This decomposition (actually its discrete counterpart) will play a key role in the projection technique that will be presented in section 3.

For sake of simplicity, it is hereafter assumed that $\mathrm{meas}(\partial\Omega_3) > 0$ so that the pressure is uniquely defined in M. If this hypothesis is not satisfied, we have to take the quotient of $L^2(\Omega)$ by constants, *i.e.* $M = L^2(\Omega)/\mathbb{R}$ (see also the proof of lemma 2.3).

We now consider the following variational problem that we call $\mathcal{P}_1$. For $f \in L^2(0,T;L^2(\Omega)^d)$, and $u_0 \in H$, find $u \in C^0(0,T;H) \cap L^2(0,T;X)$ and $p \in L^2(0,T;M)$ so that $u_{|t=0} = u_0$ and

$$\mathcal{P}_1 \begin{cases} \forall v \in X, & \left(\frac{\partial u}{\partial t}, v\right) + (\nabla\cdot u, \nabla\cdot v) + (\nabla\times u, \nabla\times v) - \int_{\partial\Omega_2} \alpha\, u \times v \cdot n \\ & \qquad + ((u^*\cdot\nabla)u, v) - (p, \nabla\cdot v) = (f, v), \\ \forall q \in M, & (\nabla\cdot u, q) = 0, \end{cases} \tag{2.9}$$

where the first equation is to be understood in the distribution sense, *i.e.* in $\mathrm{D}'(0,T)$. The equivalence between $\mathcal{P}_0$ and $\mathcal{P}_1$ is emphasized by the standard result:

PROPOSITION 2.2. *Smooth velocity and pressure fields (u,p) are solution of $\mathcal{P}_0$ if and only if they are solution to $\mathcal{P}_1$.*

Remark 2.1. The conditions on the trace, the normal trace or the tangential trace of the velocity on $\partial\Omega$ are all essential boundary conditions; they are enforced by the definition of the Hilbert space X. Note that these boundary conditions are understood in some weak sense the exact meaning of which is out of the scope of the present paper, *cf. e.g.* Lions–Magenes [20]. The condition involving the tangential components of vorticity on $\partial\Omega_2$ is a natural boundary condition. The pressure boundary condition on $\partial\Omega_3$ is natural as well. Actually, the weak formulation enforces the natural boundary condition $(\nabla\cdot u - p)_{|\partial\Omega_3} = 0$ (see also remark 3.2 below).

Remark 2.2. Note that the use of the bilinear form $(\nabla\cdot u, \nabla\cdot v) + (\nabla\times u, \nabla\times v)$ is mandatory when the boundaries $\partial\Omega_2$ and $\partial\Omega_3$, where conditions different from purely Dirichlet conditions for the velocity are prescribed, are curved. On the contrary, the more common bilinear form $(\nabla u, \nabla v)$ can be used when Dirichlet conditions are specified or when the boundaries $\partial\Omega_2$ and $\partial\Omega_3$ are flat and parallel to the Cartesian axes. Note also that the coupling between the velocity components, engendered by non purely Dirichlet boundary conditions on velocity, appears in the definition of the test functions of X.

In order to simplify the notations and put our problem in an abstract framework we define the continuous operators $A_1, A_2 : X \longrightarrow X'$ so that

$$\langle A_1 u, v\rangle = (\nabla\cdot u, \nabla\cdot v) + (\nabla\times u, \nabla\times v),$$

and

$$\langle A_2 u, v\rangle = -\int_{\partial\Omega_2} \alpha\, u \times v \cdot n + ((u^*\cdot\nabla)u, v).$$

We also define the operator $B : X \longrightarrow M$ so that

$$(Bv, q) = -(\nabla\cdot v, q)$$

for all $v \in X$ and $q \in M$. Let $B^t : M \longrightarrow X'$ the transpose of B. Concerning B, we can prove

LEMMA 2.3. *B is onto.*

Proof. The demonstration of this result is quite classical when Dirichlet conditions are enforced on velocity on the entire boundary, that is when $X = H_0^1(\Omega)^d$. The result is less known in the general case we are considering, hence we give a proof.
(a) Let us prove first that B^t is into. Let p be in the null space of B^t. For all v in X we have $\langle B^t p, v\rangle = 0$. Let us take v in $H_0^1(\Omega)^d$, and integrate by parts:

$$0 = \langle B^t p, v\rangle = -(p, \nabla\cdot v) = (\nabla p, v).$$

That is to say, $\nabla p = 0$ in $H^{-1}(\Omega)^d$, *i.e.* p is a constant (almost everywhere), in particular p (say a representative of its class of equivalence) is in $H^1(\Omega)$. As a consequence we have the following equalities for all v in X:

$$\langle B^t p, v\rangle = -(p, \nabla\cdot v) = (\nabla p, v) - \int_{\partial\Omega_3} p\, v\cdot n = -p\int_{\partial\Omega_3} v\cdot n = 0.$$

The last equality implies that p is equal to 0, for $\mathrm{meas}(\partial\Omega_3) > 0$, *i.e.* $ker\, B^t = \{0\}$.
(b) We now apply an altered version of Peetre–Tartar's lemma (see Girault–Raviart for more details [13, p. 18]). Note first that we have the inequality $|\nabla p|_{-1} \le |B^t p|_{X'}$, since

$$\begin{aligned} |\nabla p|_{-1} &= \sup_{v\in H_0^1(\Omega)^d} \frac{(\nabla p, v)}{|v|_1} \\ &= \sup_{v\in H_0^1(\Omega)^d} \frac{(p, \nabla\cdot v)}{|v|_1} \\ &\le \sup_{v\in X} \frac{(p, \nabla\cdot v)}{|v|_1} \\ &= \sup_{v\in X} \frac{\langle B^t p, v\rangle}{|v|_1}. \end{aligned}$$

Thanks to this inequality together with the inequality $c|p|_0 \le |p|_{-1} + |\nabla p|_{-1}$ (which may be found, for instance, in Girault–Raviart [13, p. 20]), we obtain

$$c|p|_0 \le |p|_{-1} + |B^t p|_{X'}, \tag{2.10}$$

from which we infer that there is a constant $c > 0$ so that

$$c|p|_0 \le |B^t p|_{X'}. \tag{2.11}$$

We prove this by contradiction. Assume that there is a sequence $\{p_n\}$ in M so that $|p_n|_0 = 1$ and $\lim_\infty |B^t p_n|_{X'} = 0$. The injection of $L^2(\Omega)$ in $H^{-1}(\Omega)$ being compact, we have a subsequence (still denoted by $\{p_n\}$) which converges in $H^{-1}(\Omega)$. The inequality (2.10) implies that the subsequence $\{p_n\}$ is a Cauchy sequence in $L^2(\Omega)$. Let p be the limit of the sequence in $L^2(\Omega)$. Since B^t is bounded, we have $\lim_\infty B^t p_n = B^t p = 0$; that is $p \in ker\, B^t$. From (a) we infer that $p = 0$, which is a contradiction to the fact that $|p_n|_0 = 1$.

(c) from the injectivity of B^t, the inequality (2.11), and the lemma 2.4 we infer that B is onto. □

An important corollary of Banach's closed range theorem is as follows.

LEMMA 2.4. *Let X and M be two Hilbert spaces, and $B \in \mathcal{L}(X, M)$. The following propositions are equivalent*

(i) $B : X \longrightarrow M$ *is onto.*

(ii) $B^t : M \longrightarrow V^0$ *is an isomorphism, where V^0 is the polar set of $V = ker\, B$, that is $V^0 = \{x' \in X',\ \forall v \in V,\ \langle x', v\rangle = 0\}$, and there is a constant $\gamma > 0$ so that*

$$\forall q \in M, \qquad |B^t q|_{X'} \ge \gamma |q|_M.$$

Proof. See *e.g.* Brezis [3, p. 29–30] or Brezzi [4]. □

Concerning A_1, we can prove

LEMMA 2.5. *Provided $\partial\Omega$ is smooth enough, A_1 is X-elliptic in the sense that there is $c > 0$ so that for all v in X we have : $\langle A_1 v, v\rangle \ge c|v|_1^2$.*

Proof. The demonstration of this result is not very well-known when boundary conditions are blended, so we give a proof (without claiming originality).
(i) First we prove that A_1 is into. If Ω is not simply connected, *i.e.* Ω is p-connected, we define p cuts $\Sigma_1, \ldots, \Sigma_p$ so that the cuts in question are smooth manifolds of dimension $d-1$, $\Sigma_i \cap \Sigma_j = \emptyset$ if $i \ne j$, and $\dot\Omega = \Omega \setminus \bigcup_{i=1}^p \Sigma_i$ is simply connected and smooth. Let u be in X and assume that $A_1 u = 0$, then $\nabla\cdot u = 0$ and $\nabla\times u = 0$ in $\dot\Omega$. Thanks to the simple connectivity of $\dot\Omega$, this means that u is the gradient of a harmonic scalar function ϕ. The boundary conditions $n\cdot u_{|\partial\Omega_1\cup\partial\Omega_2} = 0$ and $n\times u_{|\partial\Omega_3} = 0$ mean that $(\partial\phi/\partial n)_{|\partial\Omega_1\cup\partial\Omega_2} = 0$ and $\phi_{|\partial\Omega_3} = constant$, respectively. Thanks to the extension theorem of harmonic functions (*cf. e.g.* Dautray–Lions [8, Chap. II, p. 308]) we infer that ϕ is a constant in $\dot\Omega$; as a result, ϕ is constant almost everywhere in Ω. That is to say u is zero almost everywhere in Ω; hence, the class representative of u in X (in the sense of the Lebesgue measure) is zero.

(ii) Let u and v be some smooth functions X. Irrespective of any boundary condition assumed by u and v, an integration by parts yields

$$(\nabla u, \nabla v) = \langle A_1 u, v\rangle + \int_{\partial\Omega} \left[(\nabla\times u)\cdot v\times n - (\nabla\cdot u)\, v\cdot n + \frac{\partial u}{\partial n}\cdot v\right].$$

Denote by $I_{\partial\Omega}(u, v)$ the boundary integral in the right-hand side. Provided $\partial\Omega$ is smooth enough, thanks to the boundary conditions enforced on the functions of X (namely $w_{|\partial\Omega_1} = 0$, $w\cdot n_{|\partial\Omega_2} = 0$, $w\times n_{|\partial\Omega_3} = 0$) the surface integral can be bounded (after some calculus) as follows

$$I_{\partial\Omega}(u, v) \le c\int_{\partial\Omega} |u\cdot v|.$$

For other details on the way of obtaining this inequality, the reader is referred to Dautray–Lions [8, Chap. IX, p. 246]. Hence, thanks to Poincaré's inequality and the inequalities above, we infer the important result

$$c|u|_1^2 \le \langle A_1 u, u\rangle + c'\int_{\partial\Omega} |u|^2.$$

(iii) Thanks to (i), (ii) and the fact that the imbedding of $H^{1/2}(\partial\Omega)$ into $L^2(\partial\Omega)$ is compact, we can use Peetre–Tartar's lemma (as in the proof of lemma 2.3) to prove the desired inequality

$$c|u|_1^2 \leq \langle A_1 u, u\rangle.$$

Hence A_1 is elliptic on X. □

Remark 2.3. For other details on this matter the reader is referred to Girault–Raviart [13, p. 51–56].

We now turn our attention to the well-posedness of $\mathcal{P}_1$.

PROPOSITION 2.6. *$\mathcal{P}_1$ is well posed.*

Proof. Our problem can be written in the following form. For $f \in L^2(0,T;L^2(\Omega)^d)$, and $u_0 \in H$, find $u \in C^0(0,T;H) \cap L^2(0,T;X)$ and $p \in L^2(0,T;M)$ so that $u_{|t=0} = u_0$

$$\begin{cases} \dfrac{du}{dt} + A_1 u + A_2 u + B^t p = f, \\ Bu = 0. \end{cases}$$

By integration by parts we have

$$\langle A_2 u, u\rangle = -\langle A_2 u, u\rangle - (\nabla\cdot u^*, |u|^2) + \int_{\partial\Omega_{2,3}} u^*\cdot n\,|u|^2,$$

which, thanks to the hypotheses on u^*, yields $\langle A_2 u, u\rangle \geq 0$. Hence, $A_1 + A_2$ is X-elliptic. Thanks to Lions' theorem (*cf.* Brezis [3, p. 218]) and the theory of saddle point problems (*cf.* Brezzi [4]), this problem is well posed since $A_1 + A_2$ is X-elliptic and B is onto (see lemmas above). □

In the sequel we assume that u, p are smooth solutions of $\mathcal{P}_1$, and that at the initial time all the compatibility conditions implied by the required smoothness are satisfied. For instance, such conditions are satisfied if the initial datum is zero and the source terms are regularized at $t = 0$.

2.3. The spatial discretization abstract setting. Let X_h be a finite dimensional subspace of X. We equip X_h with the norm of $H^1(\Omega)^d$ and assume that X_h is an internal approximation of X. In order to build an analogy with the continuous problem we introduce $L_h = X_h$ in terms of vector space and we equip L_h with the norm of $L^2(\Omega)^d$; furthermore, we introduce X_h' the dual of X_h. Even though X_h, L_h and X_h' are identical in terms of vector spaces we make a clear difference between their norms. Likewise, we define M_h a finite dimensional subspace of M that we equip with the norm of $L^2(\Omega)$, and we assume that M_h is an internal approximation of M.

We now introduce the continuous bilinear form $b_h : X_h \times M_h \longrightarrow \mathbb{R}$ so that $b_h(v,q) = -(\nabla\cdot v, q)$ for all v in X_h and q in M_h. We associate with b_h the continuous linear operator $B_h : X_h \longrightarrow M_h$ and its transpose $B_h^t : M_h \longrightarrow X_h'$ so that for every couple (u,p) in $X_h \times M_h$ we have $(B_h u, p) = b_h(u,p)$ and $(u, B_h^t p) = b_h(u,p)$. We assume in the sequel that B_h is onto; that is to say, according to lemma 2.4,

$B_h^t : M_h \longrightarrow (ker\, B_h)^0$ is an isomorphism and there is a constant $c > 0$ (preferably independent of h) so that

$$\forall q \in M_h, \qquad |B_h^t q|_{X_h'} \geq c|q|_{M_h}. \tag{2.12}$$

Let us also introduce the continuous bilinear form $a_h : X_h \times X_h \longrightarrow \mathbb{R}$, so that for all (u,v) in $X_h \times X_h$,

$$a_h(u,v) = (\nabla\cdot u, \nabla\cdot v) + (\nabla\times u, \nabla\times v) - \int_{\partial\Omega_2} \alpha\, u\times v\cdot n + ((u^*\cdot\nabla)u, v). \tag{2.13}$$

Recall that, thanks to lemma 2.5, together with the hypotheses on u^*, a_h is X-elliptic, *i.e.*

$$\exists c > 0,\ \forall u \in X_h, \qquad a_h(u,u) \geq c|u|_X^2. \tag{2.14}$$

We associate with a_h the linear continuous operator $A_h : X_h \longrightarrow X_h'$ so that, for all $(u,v) \in X_h \times X_h$, $a_h(u,v) = (A_h u, v)$.

Let $i_{X_h} : X_h \longrightarrow X$ be the continuous injection of X_h into X, and $i_{X_h}^t$ be its transpose. Likewise we define i_{M_h} the continuous injection of M_h into M, and $i_{M_h}^t$ its transpose. We summarize the main relationships between the operators defined above in the following commutative diagram.

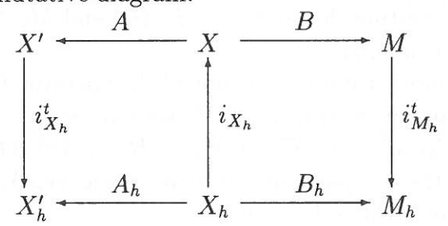

The dual diagram is obtained by taking the transpose of the operators, the dual of every space, and changing the sense of the arrows.

In the functional framework defined above, the spatially discretized time-dependent Stokes problem can be reformulated as follows. For $f \in L^2(0,T;X')$ and $u_{0,h} \in ker(B_h)$ find $u_h \in L^2(0,T;X_h)$ and $p_h \in L^2(0,T;M_h)$ so that:

$$\begin{cases} \dfrac{du_h}{dt} + A_h u_h + B_h^t p_h = i_{X_h}^t f \\ B_h u_h = 0 \\ u_{h|t=0} = u_{0,h} \end{cases} \tag{2.15}$$

where $u_{0,h} \in ker(B_h)$ is an approximation of u_0 in X_h. The discrete counterpart of the force is hereafter denoted by f_h for simplicity.

It is an easy matter to show that problem (2.15) is well posed. We hereafter assume that the solution of this semi-discretized problem converges in the appropriate sense to that of (2.9); the convergence analysis is very classical (see for instance Quarteroni–Valli [24, p. 434]). In the following we are interested only in approximating the time-dependent problem by means of a projection technique. We assume that the solution to (2.15) is as smooth as needed.

3. The fractional-step projection algorithms.

3.1. The abstract discrete setting. The functional framework as defined above is suitable for classical coupled approximations of the Stokes problem; however, in our attempt to uncouple the incompressibility constraint from the time evolution problem, we are led to introduce additional tools (see [16] for other details). We define Y_h a finite dimensional subspace of $L^2(\Omega)^d$, we equip Y_h with the norm of $L^2(\Omega)^d$, and for sake of simplicity we assume that $X_h \subset Y_h$ (in terms of vector space) and we denote by i_h the continuous injection of X_h into Y_h. Note that Y_h is an internal approximation of $L^2(\Omega)^d$, for X_h is an approximation of X and X is dense in $L^2(\Omega)^d$. Furthermore, we assume that Y_h and M_h are compatible in the sense that either Y_h is conformal in

$$H^{div}_{0,\partial\Omega_{1,2}}(\Omega) = \{v \in L^2(\Omega)^d,\ \nabla\cdot v \in L^2(\Omega),\ v\cdot n_{|\partial\Omega_{1,2}} = 0\}$$

or M_h is conformal in

$$H^1_{0,\partial\Omega_3}(\Omega) = \{q \in H^1(\Omega),\ q_{|\partial\Omega_3} = 0\}.$$

For instance, we have the trivial choice $Y_h = X_h$, but we can also choose $Y_h \subset H^{div}_{0,\partial\Omega_{1,2}}(\Omega)$; another interesting choice is $Y_h \subset L^2(\Omega)^d$ and $M_h \subset H^1_{0,\partial\Omega_3}(\Omega)$ (see farther below and [16] for other details).

We also introduce another discrete version of the operator B; we define $C_h : Y_h \longrightarrow M_h$ so that for every couple (v,q) in $Y_h \times M_h$ we have either $(C_h v, q) = -(\nabla\cdot v, q)$ if $Y_h \subset H^{div}_{0,\partial\Omega_{1,2}}(\Omega)$ or $(C_h v, q) = (v, \nabla q)$ if $M_h \subset H^1_{0,\partial\Omega_3}(\Omega)$. Of course this definition makes sense thanks to the compatibility we require between Y_h and M_h. The relation between B_h and C_h is brought to light by

PROPOSITION 3.1. *C_h is an extension of B_h, and $i_h^t C_h^t = B_h^t$; in other words we have the following commutative diagrams:*

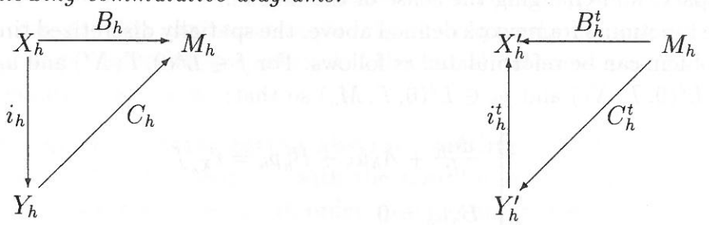

Proof. (a) Assume $Y_h \subset H^{div}_{0,\partial\Omega_{1,2}}(\Omega)$. For all (v,q) in $X_h \times M_h$, we have $(C_h i_h v, q) = -(\nabla\cdot(i_h v), q) = -(\nabla\cdot v, q) = (B_h v, q)$ since $X_h \subset Y_h$; that is to say, $C_h i_h v = B_h v$ for all $v \in X_h$.
(b) Assume $M_h \subset H^1_{0,\partial\Omega_3}(\Omega)$. For all (v,q) in $X_h \times M_h$, we have $(C_h i_h v, q) = (i_h v, \nabla q) = (v, \nabla q) = -(\nabla\cdot v, q) = (B_h v, q)$ since $X_h \subset Y_h$ and $q_{|\partial\Omega_3} = 0$; that is to say, $C_h i_h v = B_h v$ for all $v \in X_h$.
(c) By taking the transpose of $C_h i_h = B_h$ we obtain $i_h^t C_h^t = B_h^t$. □

Recall that we have assumed that B_h is onto; as a consequence, C_h is also necessarily onto for C_h is an extension of B_h. One consequence of this (together with (ii) of lemma 2.4) is that $|C_h^t q|_{Y_h}$ is a norm; this norm is hereafter denoted by $|q|_{M_h^1} = |C_h^t q|_{Y_h}$

and we denote by M_h^1 the vector space M_h equipped with this norm. The null space of C_h playing an important role in the sequel we set $H_h = ker\, C_h$. The definitions above enable us to build a discrete counterpart of the classical decomposition $L^2(\Omega)^d = H \oplus \nabla(H^1_{0,\partial\Omega_3}(\Omega))$ stated in proposition 2.1.

COROLLARY 3.1. *We have the orthogonal decomposition:*

$$Y_h = H_h \oplus C_h^t(M_h^1). \tag{3.1}$$

Proof. Let $f \in Y_h$, look for $p \in M_h$ so that $(C_h^t p, C_h^t q) = (f, C_h^t q)$ for all $q \in M_h$. This problem has a unique solution thanks to Lax–Milgram's theorem (for $|\cdot|_{M_h^1}$ is a norm!). We have $|p|_{M_h^1} \le |f|_{Y_h}$. One easily verifies that $u = f - C_h^t p$ is in H_h. □

3.2. The abstract fractional-step projection scheme. Introduce a partition of the time interval $[0,T]$: $t^k = k\delta t$ for $0 \le k \le K$ where $\delta t = T/K$, and define two series of approximate velocities $\{\tilde u_h^k \in X_h\}$ and $\{u_h^k \in Y_h\}$ and one series of approximate pressures $\{p_h^k \in M_h\}$ so that

$$\begin{cases} \dfrac{\tilde u_h^{k+1} - i_h^t u_h^k}{\delta t} + A_h \tilde u_h^{k+1} = f_h^{k+1} - B_h^t p_h^k \end{cases} \tag{3.2}$$

and

$$\begin{cases} \dfrac{u_h^{k+1} - i_h \tilde u_h^{k+1}}{\delta t} + C_h^t(p_h^{k+1} - p_h^k) = 0 \\ C_h u_h^{k+1} = 0 \end{cases} \tag{3.3}$$

The series $\{u_h^k\}$ is initialized by $u_h^0 = u_{0,h}$ and assuming that $p_h \in C(0,T;M_h)$ the series $\{p_h^k\}$ is initialized by $p_h^0 = p_{h|t=0}$.

Remark 3.1. The problem (3.2) is well posed since A_h is X_h-elliptic. The problem (3.3) is also well posed thanks to corollary 3.1: indeed the couple $(u_h^{k+1}, \delta t(p_h^{k+1} - p_h^k))$ is the decomposition of $\tilde u_h^{k+1}$ in $H_h \oplus C_h^t(M_h^1)$; *i.e.*, $u_h^{k+1} = P_{H_h}\tilde u_h^{k+1}$ where P_{H_h} is the orthogonal projection of Y_h onto H_h.

Remark 3.2. The discretized equation (3.2) enforces weakly the natural boundary condition $(\nabla\cdot\tilde u_h^{k+1} - p_h^k)_{|\partial\Omega_3} = 0$ (see also remark 2.1 above).

Remark 3.3. The original Chorin–Temam algorithm does not contain $B_h^t p_h^k$ in the right-hand side of the (3.2); in the sequel we refer to it as the nonincremental algorithm, whereas the algorithm presented here is referred to as the incremental one. Most of what is said in this paper applies also to the original nonincremental projection algorithm. In short, both algorithms converge, but the incremental one has a better rate of convergence than the nonincremental one (see [15]).

Denote by $e_h^k = u_h(t^k) - u_h^k$, $\tilde e_h^k = u_h(t^k) - \tilde u_h^k$ and $\epsilon_h^k = p_h(t^k) - p_h^k$ the error functions; the ability of the solution to (3.2)–(3.3) to approximate that of (2.15) is given by

THEOREM 3.1. *If the solution to (2.15) is such that $u_{h,tt} \in L^2(0,T;L_h)$ and $p_{h,t} \in L^2(0,T;M_h^1)$ and if the series $\{u_h^k\}$ and $\{p_h^k\}$ are initialized so that $|u_h^0 - u_{0,h}|_L \le c\delta t$*

and $|p_h^0 - p_{h|t=0}|_{M_h^1} \leq c$ *then we have the following error estimate:*

$$\sup_{0\leq t^k\leq T} |e_h^k|_0 + \left[\delta t \sum_{k=0}^{K} |\tilde{e}_h^k|_X^2\right]^{1/2} \leq c\delta t. \tag{3.4}$$

Furthermore, if $u_{h,ttt} \in L^2(0,T;L_h)$, $p_{h,t} \in L^2(0,T;M_h^1)$, $|\epsilon_h^0|_0 \leq c(\delta t)^2$, $|\epsilon_h^0|_{M_h^1} \leq c\delta t$ *then*

$$\left[\delta t \sum_{k=0}^{K} |\epsilon_h^k|_M^2\right]^{1/2} \leq c\delta t. \tag{3.5}$$

The proof of this result can be found in Guermond [15]. An extension of this result to the non-incremental technique in the continuous case is reported in Rannacher [25]. The reader is also referred to Rannacher [25] for an interesting interpretation of the projection technique as a pressure stabilization technique. The error estimates given above are not, in principle, completely satisfactory, since they depend on the regularity of the discrete solution $(u_h(t), p_h(t))$. Actually, the regularity in question solely depends on the spatial approximation technique and on the regularity of the solution of the continuous problem (2.9). Obtaining regularity in time on $(u_h(t), p_h(t))$ from that of $(u(t), p(t))$ is standard (though possibly not straightforward) on spatial approximation of Stokes-like time dependent problems (*i.e.* constrained parabolic problems) and out of the scope of the present paper.

In practice it is not very convenient to solve the problem as presented here. Actually, the projected velocity u_h^k can be eliminated from the algorithm as follows (see [16]). Replace u_h^k in (3.2) by its definition which is given by (3.3) at the time step t^k; note that $i_h^t C_h^t = B_h^t$, as already mentioned. In (3.3), u_h^{k+1} is eliminated by applying C_h to the first equation and by noting that C_h is an extension of B_h. The algorithm which should be implemented reads, for $k \geq 1$,

$$\frac{\tilde{u}_h^{k+1} - \tilde{u}_h^k}{\delta t} + A_h \tilde{u}_h^{k+1} = f_h^{k+1} - B_h^t(2p_h^k - p_h^{k-1}), \tag{3.6}$$

and

$$C_h C_h^t (p_h^{k+1} - p_h^k) = \frac{B_h \tilde{u}_h^{k+1}}{\delta t}. \tag{3.7}$$

Remark 3.4. At this point one may think that $C_h C_h^t$ acts like a preconditioner of the Uzawa operator $B_h(1 - \delta t A_h)^{-1} B_h^t$. Indeed, this impression in not quite correct for three reasons. First, it is shown in [17] that, in the mere algebraic sense, $C_h C_h^t$ is not a preconditioner of the Uzawa operator, unless δt is extremely small (a condition more stringent than the explicit-type condition on δt is required). Second, if $C_h C_h^t$ were used as a preconditioner within a one step Picard-like loop, the pressure problem that should logically be solved is $C_h C_h^t (p_h^{k+1} - 2p_h^k + p_h^{k-1}) = B_h \tilde{u}_h^k / \delta t$. Third, the projection algorithm described above is not a preconditioned one step Picard-like loop, for were it be, the velocity should be corrected accordingly after the pressure p_h^{k+1} is calculated. See also Rannacher's interpretation [25]

Remark 3.5. Higher accuracy in time can be obtained if we replace the two-level backward Euler step of first order by a backward three-level Euler step of second order as follows

$$\frac{3\tilde{u}_h^{k+1} - \tilde{u}_h^k - i_h^t(3u_h^k - u_h^{k-1})}{2\delta t} + A_h \tilde{u}_h^{k+1} = f_h^{k+1} - B_h^t p_h^k, \tag{3.8}$$

and

$$\begin{cases} \dfrac{3u_h^{k+1} - u_h^k - i_h(3\tilde{u}_h^{k+1} - \tilde{u}_h^k)}{2\delta t} + C_h^t(p_h^{k+1} - p_h^k) = 0, \\ C_h u_h^{k+1} = 0. \end{cases} \tag{3.9}$$

Of course, the algorithm can be implemented in a more convenient form by eliminating the end-of-step velocity, as follows:

$$\frac{3\tilde{u}_h^{k+1} - 4\tilde{u}_h^k + \tilde{u}_h^{k-1}}{2\delta t} + A_h \tilde{u}_h^{k+1} = f_h^{k+1} - B_h^t(2p_h^k - p_h^{k-1}), \tag{3.10}$$

and

$$C_h C_h^t (p_h^{k+1} - p_h^k) = \frac{B_h^t(3\tilde{u}_h^{k+1} - \tilde{u}_h^k)}{2\delta t}. \tag{3.11}$$

It is shown in [15] that for a fixed mesh size h, this algorithm is unconditionnaly stable and yields second order accuracy in the norms used in (3.4) and (3.5) provided A_h is self-adjoint (that is $u^* = 0$). Numerical tests have shown (unfortunately) that there is only conditional stability if the self-adjointness hypothjesis is not satisfied. The proof in [15] gives a bound on the error of the form $c(h)(\delta t)^2$, but it produces an unrealistic bound on the dependence of $c(h)$ with respect to h; in this sense the proof in question is probably not optimal. However, in practice $c(h)$ varies very slowly with respect to h (*cf.* numerical experiments in [15]).

The description of the algorithms above is somewhat abstract (hence powerful); we now show how they can be implemented in practice in two different contexts.

3.3. The projection step as a Darcy problem. Theoretically it is not necessary to consider nonhomogeneous values of pressure on $\partial\Omega_3$, for we can invoke some smooth lifting of the pressure so that the new unknown pressure satisfies a homogeneous boundary condition. This theoretical argument is perfectly correct and we should be satisfied with it; on the other hand, the practical application of this principle may seem counter-intuitive and may perhaps lead one to attempt to enforce the nonhomogeneous pressure boundary condition at the projection step (which is wrong!). We assume in this section that the pressure should satisfy a nonhomogeneous Dirichlet condition on $\partial\Omega_3$, namely,

$$p_{|\partial\Omega_3} = p_{\partial\Omega_3}. \tag{3.12}$$

The definition of our functional framework remains unchanged. The only thing that changes is the right-hand side of the momentum equation in variational form (2.9), which should be replaced by

$$(f,v) - \int_{\partial\Omega_3} p_{\partial\Omega_3}\, v\cdot n. \tag{3.13}$$

As a consequence, the discrete problem (3.2) is modified only in the right-hand side of the discrete momentum equation. Namely, the linear form f_h must be replaced by $g_h : X_h \longrightarrow X_h'$ so that, for all $v_h \in X_h$, $(g_h, v_h) = (f, v_h) - \int_{\partial\Omega_3} p_{\partial\Omega_3}\, v_h\cdot n$. The projection algorithm as described above remains unchanged provided f_h^{k+1} is replaced by g_h^{k+1} in the viscous step (3.2).

To be more explicit we now show how the method should be implemented in the particular situation $Y_h = X_h$. In such a case no distinction is needed between the operators B_h and C_h. For an example of practical implementation of this framework, the reader is referred to Gresho and Chan [14].

The viscous step amounts to looking for $\tilde{u}_h^{k+1}$ in X_h so that, for all $v_h \in X_h$, we have

$$\left(\frac{\tilde{u}_h^{k+1} - u_h^k}{\delta t}, v_h\right) + a_h(\tilde{u}_h^{k+1}, v_h) = (f^{k+1}, v_h) + (p_h^k, \nabla\cdot v_h) - \int_{\partial\Omega_3} p_{\partial\Omega_3}^k\, v_h\cdot n. \tag{3.14}$$

The projection step consists in looking for u_h^{k+1} in X_h and p_h^{k+1} in M_h so that

$$\begin{cases} \forall v_h \in X_h, \quad \left(\dfrac{u_h^{k+1} - \tilde{u}_h^{k+1}}{\delta t}, v_h\right) - ((p_h^{k+1} - p_h^k), \nabla\cdot v_h) = 0, \\ \forall q_h \in M_h, \quad (\nabla\cdot u_h^{k+1}, q_h) = 0. \end{cases} \tag{3.15}$$

Remark 3.6. In this framework the pressure boundary condition on $\partial\Omega_3$ is naturally enforced in the viscous step (3.14). In the projection step no essential boundary condition on the pressure is enforced; though in the weak sense the projection step naturally enforces the (always) homogeneous boundary condition $(p_h^{k+1} - p_h^k)_{|\partial\Omega_3} = 0$. Actually, (3.15) can be understood as a discrete approximation of a Darcy problem.

Remark 3.7. Note that in the projection step the velocity u_h^{k+1} is sought in X_h. As a result, u_h^{k+1} satisfies all the essential boundary conditions enforced by X_h. In some sense this may seem surprising, even paradoxical, for the projection step should be the discrete counterpart of the continuous one, in which the projected velocity belongs to H, and therefore must satisfy the boundary condition $u\cdot n_{|\partial\Omega_{1,2}} = 0$. Indeed, there is no contradiction for, X being dense in $H^{div}_{0,\partial\Omega_{1,2}}(\Omega)$, any approximation X_h of X is also an approximation of $H^{div}_{0,\partial\Omega_{1,2}}(\Omega)$; that is, the projected velocity can be approximated perfectly by elements of X_h.

Remark 3.8. It is shown in [16] that this approximation is optimal for finite element spatial discretizations in the sense that the pressure operator associated to the projection step has an optimal condition number. This result is likely to be no longer true when spectral approximations are used. Optimality can be recovered if we reformulate (3.3) so that the test functions satisfy $v\cdot n_{|\partial\Omega_{1,2}} = 0$. This can be done by

choosing Y_h as being a subspace of $H^{div}_{0,\partial\Omega_{1,2}}(\Omega)$. In this context, u_h^{k+1} in (3.3) being sought in Y_h satisfies only $u_h^{k+1}\cdot n_{|\partial\Omega_{1,2}} = 0$. This technique is optimal for spectral approximations (see [1] for examples of such approximations), since for some cases of this class of approximations it is possible to show that the pressure operator $C_h C_h^t$ is better conditioned than $B_h B_h^t$. Indeed this approach constitutes a second possible implementation. We just mention it and will not go any further in the details (see [16] for other details on this matter). For finite element approximations the condition numbers of both operators are equivalent. As a result, the first approach (*i.e.* $Y_h = X_h$ and $C_h = B_h$) may be recommended for finite element discretizations; one advantage of this approach being that the operators (the matrices also) B_h and C_h involved in (3.2) and (3.3) are identical.

In practice we do not manipulate operators but matrices; that is, we choose particular bases of X_h and M_h. Each of these choices yields a mass matrix I_h and a matrix associated with the divergence operator, say B_h. For a velocity field u_h in X_h and a pressure field p_h in M_h, we denote by U and P the vectors of the components of u_h and p_h in the bases in question. In this context, the projection step as described above yields the following linear system in terms of the pressure unknowns

$$B_h I_h^{-1} B_h^t (P^{k+1} - P^k) = \frac{B_h \tilde{U}^{k+1}}{\delta t}. \tag{3.16}$$

The matrix of the linear system associated to the pressure equation involves the inverse of the mass matrix. In practice the presence of I_h^{-1} may hamper the practicability of the present approach in some circumstances. For instance, for finite element approximations the mass matrix is not diagonal, and the exact determination of the matrix of the pressure problem may become computationally very expensive, especially when a large number of unknowns are involved. In practice, alternative approaches consist in (diagonally) lumping the mass matrix (*cf.* Gresho and Chan [14, part II] or Quartapelle [23, pp. 191–201]). Though this technique may work, no stability result has yet been proven.

It is the purpose of the next section to show that the mass matrix problem may be circumvented if we adequately choose the auxiliary space Y_h in which the velocity is projected.

3.4. The projection step as a Poisson problem. We now chose M_h as an internal approximation of $H^1_{0,\partial\Omega_3}(\Omega)$ (recall that in the previous sections we only required $M_h \subset L^2(\Omega)$). We also chose $Y_h = X_h + \nabla M_h$; note that this definition makes sense for M_h being a subspace of $H^1_{0,\partial\Omega_3}(\Omega)$, ∇M_h is in $L^2(\Omega)^d$, that is to say, Y_h is a subspace of $L^2(\Omega)^d$ as required by the theory developed above.

In this alternative framework the viscous step amounts to looking for $\tilde{u}_h^{k+1}$ in X_h so that, for all $v_h \in X_h$, we have

$$\frac{(\tilde{u}_h^{k+1}, v_h) - (u_h^k, v_h)}{\delta t} + a_h(\tilde{u}_h^{k+1}, v_h) = (f^{k+1}, v_h) + (p_h^k, \nabla\cdot v_h) - \int_{\partial\Omega_3} p_{\partial\Omega_3}^k\, v_h\cdot n. \tag{3.17}$$

Note that $\tilde{u}_h^{k+1}$ and u_h^k are not approximated in the same space. Furthermore, the projection step takes the form: look for u_h^{k+1} in Y_h and p_h^{k+1} in M_h so that

$$(3.18)\qquad \begin{cases} \forall v_h \in Y_h, \quad \left(\dfrac{u_h^{k+1} - i_h\tilde{u}_h^{k+1}}{\delta t}, v_h\right) + (\nabla(p_h^{k+1} - p_h^k), v_h) = 0, \\ \forall q_h \in M_h, \quad (u_h^{k+1}, \nabla q_h) = 0. \end{cases}$$

At first glance this formulation seems strange, even awkward, for Y_h is not a classical space. Actually, the usefulness of Y_h is emphasized by the following

PROPOSITION 3.2. *The projection step (3.18) is equivalent to the problem: look for p_h^{k+1} in M_h so that*

$$(3.19)\qquad \forall q_h \in M_h, \quad (\nabla(p_h^{k+1} - p_h^k), \nabla q_h) = -\frac{(\nabla\cdot\tilde{u}_h^{k+1}, q_h)}{\delta t},$$

and set

$$(3.20)\qquad u_h^{k+1} = \tilde{u}_h^{k+1} - \delta t\nabla(p_h^{k+1} - p_h^k).$$

Proof. This an easy consequence of lemma 3.3 that follows. □

LEMMA 3.3. *C^t is the restriction of ∇ to M_h.*

Proof. For all (v, q) in $Y_h \times M_h$, we have $(C_h^t q, v) = (\nabla q, v)$; that is to say $(C_h^t q - \nabla q, v) = 0$. But ∇q is in Y_h by definition and $C_h^t q$ is in Y_h' (= Y_h in terms of vector space); hence $C_h^t q = \nabla q$. □

Remark 3.9. In the new framework, the projection step amounts to solving a discrete Poisson problem with homogeneous natural Neumann boundary condition on $\partial\Omega_1 \cup \partial\Omega_2$ and homogeneous essential Dirichlet boundary condition on $\partial\Omega_3$. This type of discrete problem is very classical and the solution of the linear system associated with it has been subject to an enormous amount of research. Accurate and fast solvers of this problem are available.

Remark 3.10. Note that u_h^{k+1} belongs to $X_h + \nabla M_h$ which is a subset of $L^2(\Omega)^d$. Strictly speaking, u_h^{k+1} needs not to be divergence free, for there is no reason for $\nabla\cdot\tilde{u}_h^{k+1}/\delta t$ to be equal to $\nabla^2(p_h^{k+1} - p_h^k)$. For instance, if P_1 finite elements are used for approximating the pressure, the Laplacian of the pressure increment is a $H^{-1}(\Omega)$ measure, whereas the divergence of the provisional velocity is in $L^2(\Omega)$. However, we can prove that as the mesh is refined (*i.e.* the approximation parameter h tends to zero), u_h^{k+1} converges weakly in $L^2(\Omega)^d$ to some divergence free vector field.

Remark 3.11. Since the homogeneous Dirichlet condition on $\partial\Omega_3$ may seem unnatural (or inaccurate), it may be a temptation to try to solve the projection problem by enforcing the increment of pressure $p_h^{k+1} - p_h^k$ on $\partial\Omega_3$ to be equal to $p_{\partial\Omega_3}(t^{k+1}) - p_{\partial\Omega_3}(t^k)$. This is an error; this way of doing leads to an algorithm which not only is no longer unconditionally stable, but also is no longer a projection scheme, for it cannot ensure $|u_h^{k+1}|_0 \leq |\tilde{u}_h^{k+1}|_0$. Actually, the correct boundary condition on the pressure is *naturally* enforced at the viscous step through the surface integral on $\partial\Omega_3$. The reader who

is more concerned by physical considerations than by mathematical arguments may convince himself by thinking of the nonhomogeneous pressure boundary condition as a driving force; hence, it should be enforced in the momentum equation, and not in the projection step whose job is to satisfy the kinematic constraint $\nabla\cdot u = 0$.

Remark 3.12. As already mentioned above, the end-of-step velocity can be eliminated in practice. Hence the weird velocity space Y_h is never used in practice.

4. An approximation of the Navier–Stokes equations.

We now turn our attention to the Navier–Stokes equations. We do not pretend to give here a complete analysis of this very difficult problem (for instance, the uniqueness of the solution in 3D is still, in general, an open question... see *eg.* Temam [27]). We will admit the existence of a regular, smooth solution to our problem, though the existence of such solution is debatable (see for instance the series of papers by Heywood and Rannacher [18]). The aim of this section is to show how the algorithm presented above can be implemented to build approximations of the solutions to Navier–Stokes equations. Furthermore, we indicate (recall) a possibility of treating the nonlinear convective term so that the resulting algorithm is unconditionally stable if either meas$(\partial\Omega_3) = 0$ or the boundary $\partial\Omega_3$ is such that the flow satisfies $u\cdot n_{|\partial\Omega_3} \geq 0$.

4.1. A time-dependent, unconditionally stable approximation. For sake of simplicity, we still assume that the problem is supplemented with homogeneous boundary conditions as described in (2.2) and is approximated in space so that we are now interested in solving the following time-dependent, spatially discretized, Navier–Stokes problem. For $f \in L^2(0,T;X')$ and $u_{0,h} \in ker(B_h)$ find $u_h \in L^2(0,T;X_h)$ and $p_h \in L^2(0,T;M_h)$ so that:

$$(4.1)\qquad \begin{cases} \dfrac{du_h}{dt} + A_h^v u_h + D_h(u_h,u_h) + B_h^t p_h = i_{X_h}^t f \\ B_h u_h = 0 \\ u_{h|t=0} = u_{0,h} \end{cases}$$

where A_h^v represents only the viscous contribution to the operator, namely, A_h^v is the linear continuous operator associated with the bilinear form $a_h^v : X_h \times X_h \longrightarrow \mathbb{R}$, so that for all (u,v) in $X_h \times X_h$,

$$(4.2)\qquad a_h^v(u,v) = (\nabla\cdot u, \nabla\cdot v) + (\nabla\times u, \nabla\times v) - \int_{\partial\Omega_2} \alpha\, u\times v\cdot n.$$

In (4.1) $u_{0,h} \in ker(B_h)$ is an approximation of u_0. The bilinear operator $D_h : X_h \times X_h \longrightarrow X_h'$ is defined as follows:

$$(4.3)\quad \forall\,(u_h,v_h,w_h) \in (X_h)^3, \quad \langle D_h(u_h,v_h),w_h\rangle = ((u_h\cdot\nabla)v_h, w_h) + \frac{1}{2}(\nabla\cdot u_h, v_h\cdot w_h),$$

where $u\cdot v$ stands for the Euclidean scalar product in $\mathbb{R}^d$. Recall that thanks to the fact that $d \leq 4$, the definition of D_h makes sense (see *e.g.* Girault–Raviart [13, p. 284]

for details). Note that if X_h were a space of divergence free vector fields, we would have $\langle D_h(u_h, v_h), w_h\rangle = ((u_h\cdot\nabla)v_h, w_h)$; as a result, D_h is a consistent approximation of the usual nonlinear convection term, since the divergence of u_h is expected to be small as the mesh is refined. Furthermore we have the following important property.

PROPOSITION 4.1. *Let u_h be in X_h. Provided we have either meas$(\partial\Omega_3) = 0$ or $u_h\cdot n_{|\partial\Omega_3} \geq 0$, for all v_h in X_h the following inequality holds*

$$\langle D_h(u_h, v_h), v_h\rangle \geq 0. \tag{4.4}$$

Proof. Let $(u_h, v_h, w_h) \in (X_h)^3$; by integration by parts we have

$$\int_\Omega [(u_h\cdot\nabla)v_h]\cdot w_h = -\int_\Omega [(u_h\cdot\nabla)w_h]\cdot v_h - (\nabla\cdot u_h, v_h\cdot w_h) + \int_{\partial\Omega_3} u_h\cdot n\,(v_h\cdot w_h).$$

This implies

$$\langle D_h(u_h, v_h), v_h\rangle = \frac{1}{2}\int_{\partial\Omega_3} u_h\cdot n\,|v_h|^2$$

which, thanks to the hypotheses on either $u_h\cdot n_{|\partial\Omega_3}$ or $\partial\Omega_3$, yields the desired result. □

Thanks to this treatment of the nonlinear term we have the following stability result on the solution u_h, which mimics that of the continuous one (the discrete body force is hereafter denoted by f_h for simplicity).

PROPOSITION 4.2. *The solution to the spatially discretized Navier–Stokes problem (4.1) satisfies:*

$$c_1 \sup_{0\leq t\leq T} |u_h(t)|_0^2 + c_2\int_0^T |u_h|_1^2\,dt \leq |u_{0,h}|_0^2 + \int_0^T |f_h|_{-1}^2\,dt. \tag{4.5}$$

Proof. Take the inner product of the momentum equation with u_h, apply the ellipticity inequality (*cf.* lemma 2.5) together with the inequality (4.4), and integrate in time between 0 and t. □

Remark 4.1. Note that the treatment of the nonlinear term described above is frequently used in textbooks along with the hypothesis meas$(\partial\Omega_3) = 0$. Without pretending the originality we point out the fact that the present procedure can also be used for canal flows or other forms of flows with an "open" boundary, provided the "open" boundary in question is located downstream, far enough of any recirculatory zone, so that the condition $u_h\cdot n_{|\partial\Omega_3} \geq 0$ is guaranteed.

4.2. An unconditionally stable semi-implicit projection scheme. We now show how the projection algorithm presented above can be implemented to approximate the solution to the time-dependent but space-discretized Navier–Stokes problem considered in the previous section.

Initialize the algorithm by setting $u_h^0 = u_{0,h}$ and by finding an approximation to the initial p_h^0 by means of one step of the nonincremental algorithm with a very small time step $(\delta t)_{start} \ll \delta t$ or from some analytically known solution; moreover, starting

from u_h^0 and p_h^0, make one step of the incremental algorithm with δt to get $\tilde{u}_h^1$ and p_h^1 (many other alternatives are possible). Then for each time step $k \geq 1$ look for $\tilde{u}_h^{k+1}$ in X_h so that

$$\frac{\tilde{u}_h^{k+1} - \tilde{u}_h^k}{\delta t} + A_h^v\tilde{u}_h^{k+1} + D_h(\tilde{u}_h^k, \tilde{u}_h^{k+1}) = f_h^{k+1} - B_h^t(2p_h^k - p_h^{k-1}), \tag{4.6}$$

and find p_h^{k+1} in M_h so that

$$C_h C_h^t(p_h^{k+1} - p_h^k) = \frac{B_h\tilde{u}_h^{k+1}}{\delta t}. \tag{4.7}$$

Remark 4.2. Note that the convective term has been linearized so that the resulting time integration scheme is semi-implicit. However, thanks to the inequality (4.4) in proposition 4.1, the algorithm is unconditionally stable in the sense that we have:

PROPOSITION 4.3. *The solution produced by the semi-implicit fractional-step projection algorithm satisfies:*

$$c_1 \sup_{0\leq t^k\leq T} |\tilde{u}_h(t)|_0^2 + c_2\delta t\sum_{k=0}^K |\tilde{u}_h^k|_1^2 \leq |u_{0,h}|_0^2 + (\delta t)^2|p_h^0|^2 + \delta t\sum_{k=0}^K |f_h^k|_{-1}^2. \tag{4.8}$$

The complete convergence analysis with respect to both time and space has been done by the authors but is not reported here, since it does not bring significant additional light on the practical implementation of this scheme.

5. Numerical tests and discussions.

5.1. Spatial discretization and finite element equations. The unconditionally stable fractional-step method based on the Poisson equation for pressure described in the previous section has been implemented using P_1-iso-P_2/P_1 finite element triangular meshes. Unstructured Delaunay grids for the two-dimensional test problems have been generated by means of the procedure due to Rebay [26]. This method is simple, efficient and very convenient for the implementation of adaptive strategies of local refinement. Here it has been used to obtain nonuniform coarse grids with smaller triangles in regions of larger local relative error for speed according to a previously computed solution. A fine mesh is then obtained from the coarse one by splitting each coarse triangle into four equal small triangles introducing the mid-side nodes on all sides of the coarse mesh.

The integration over the triangles is performed by means of numerical quadrature using a three-point Gauss formula. This assures the exact evaluation of all scalar products including those which involve the nonlinear convection term. The values of the Jacobian determinant and of the weighting function derivatives at Gauss points of all elements are evaluated once an for all at the beginning of the calculation and stored in arrays for subsequent use.

The unconditionally stable algorithm requires to solve large sparse linear systems of algebraic equations for both the velocity and the pressure. The linear systems

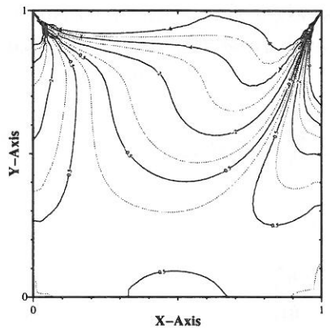

FIG. 1. *Vorticity field on a coarse uniform mesh, $R = 100$.*

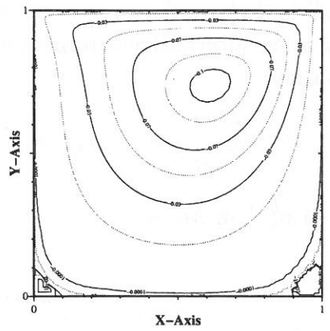

FIG. 2. *Streamlines on a coarse uniform mesh, $R = 100$. Note oscillations due to lack of refinement.*

for the velocity components are nonsymmetric and change at each time level, while that for the pressure Poisson problem is symmetric and does not depend on time. The solution of these systems is calculated by direct methods using the SPARSPAK library. More precisely, we have used the solution method most suitable for unstructured finite element problems, which minimizes storage requirements by an internal reordering the unknowns obtained by means of the one-way dissection algorithm of George [10], see also [11, p. 226].

We note that, when Dirichlet conditions are prescribed for velocity on the entire boundary, the matrix of the nonsymmetric linear system in the first step is the same for both velocity components. In this case, it is possible to perform only one (non-symmetric) factorization per time step, instead of two (resp. three) for problems in two (resp. three) dimensions. In any case, at each time step three substitutions are required in two dimensions (four substitutions in three dimensions).

The Poisson problem for pressure can be solved on the coarse mesh using P_1 polynomial interpolation on the coarse mesh. In the present implementation of the method the pressure problem is actually formulated and solved on the fine mesh, but the refined pressure solution is smoothed at each time step by interpolating the pressure values at mid-side nodes from the values at the nodes of the coarse mesh.

5.2. The driven cavity problem. The first test problem is the driven cavity introduced by Burggraf [5]. The fluid domain is a unit square and the velocity boundary conditions are of zero velocity on the entire boundary except for the upper side of the square where the tangential velocity is equal to 1; of course, the velocity at the corner nodes is fixed to zero to avoid inflow and outflow of the fluid through the first two vertical sides near the corners. The Neumann problem for the pressure is singular and, to have a unique solution, the pressure value at the midpoint of the bottom side has been fixed to zero.

The solution for a Reynolds number $R = 100$ has been calculated first on a uniform mesh of $2 \times 20 \times 20$ coarse triangles ($2 \times 40 \times 40$ fine triangles). The corresponding

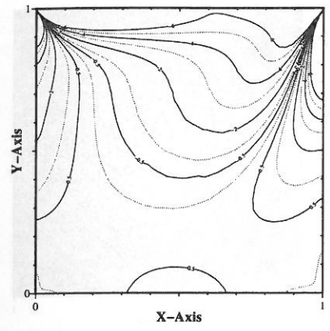

FIG. 3. *Vorticity field on locally refined mesh, $R = 100$.*

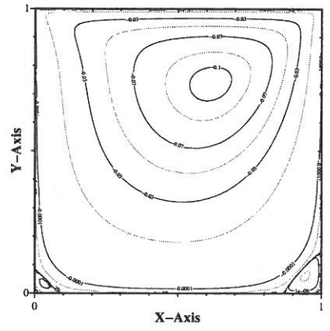

FIG. 4. *Streamlines on locally refined mesh, $R = 100$.*

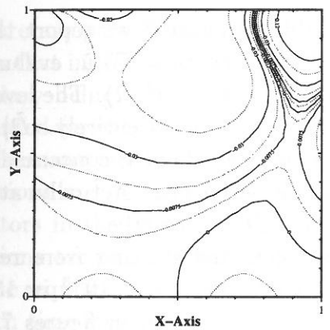

FIG. 5. *Pressure field, $R = 100$.*

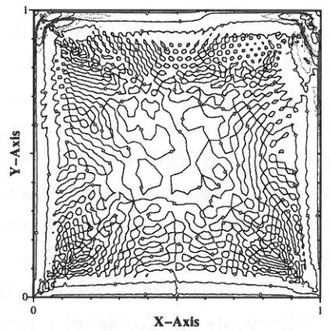

FIG. 6. *Level lines of the weak divergence of $\tilde{u}$, $R = 100$.*

vorticity ω and stream function ψ are obtained from the velocity field $\tilde{u}_h^{k+1}$ by solving a mass matrix problem and a Dirichlet problem, respectively. The solutions are given in figures 1 and 2 and are in a fully satisfactory agreement with the reference solution [12]. We emphasize that in the proposed method the value of the time step has no stability restriction: we have verified the numerical stability of the fractional-step algorithm up to $\delta t = 10^3$.

The vorticity field near the corner being sensitive to the size of the considered mesh, we have calculated the solution for $R = 100$ on an unstructured finer mesh with a nonuniform distribution of the triangles near the four corners of the cavity. This mesh consists in a total of ≈ 8800 (fine) elements for ≈ 4500 nodes, and is the same used also at higher values of R. The level curves of ω shown in figure 3 are now very smooth even in the two corner regions where the vorticity is characterized by a well known singular behaviour.

The level curves of the pressure field displayed in figure 5 are virtually undistinguishable from those provided by the penalty method of the FIDAP program (*cf.* [21]).

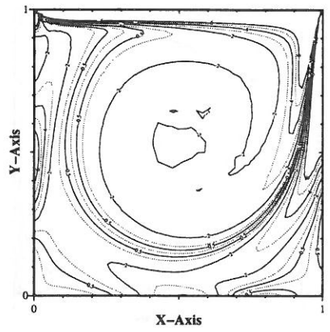

FIG. 7. *Vorticity field for* $R = 1000$.

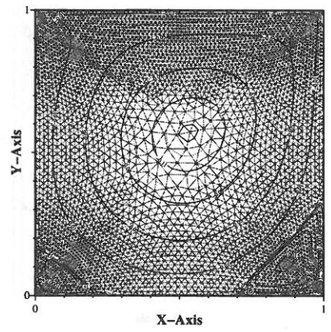

FIG. 8. *Mesh + Streamlines for* $R = 1000$.

No spatial oscillation is present in the pressure field. In figure 6 we report the level curves (values $0, \pm 0.05, \pm 0.1, \pm 0.2, \pm 0.5$) of the divergence $\tilde{D} = \nabla \cdot \tilde{u}$, evaluated by solving the mass matrix problem $(\tilde{D}, q) = (\nabla \cdot \tilde{u}, q), \forall q \in M_h \subset H^1(\Omega)$. The level curve $\tilde{D} = 0$ has a behaviour like a Peano curve filling the cavity almost entirely. $|\tilde{D}| > 10^{-2}$ only in the regions of the two upper corners; this means that (if one is concerned by this result) more iterations toward steady state should be performed. Actually, at steady state (if reached someday) we have $B_h \tilde{u}_h^{\infty} = 0$; that is $\tilde{D} = 0$ strictly.

The steady solution for $R = 1000$ has been calculated starting from rest with $\delta t = 0.5$ and reaching a relative difference $|\tilde{u}_h^{k+1} - \tilde{u}_h^k|_0 / |\tilde{u}_h^{k+1}|_0 < 10^{-3}$ in 138 time steps. The plots of the level curves for both ω and ψ are given in figures 7 and 8. The streamlines are in perfect agreement with those of the reference solution [12]; the same applies for the vorticity contours except for some wiggles in the central zone of the cavity where the employed mesh is coarsest, while the benchmark solution was calculated on a uniform 129×129 grid.

The steady solutions for $R = 3200$ has been then obtained starting from the $R = 1000$ solution and performing ≈ 100 time steps with $\delta t = 0.1$, and similarly the solution for $R = 5000$. The streamlines of these solutions are given in figures 9 and 10; they compare very well with the reference solutions [12] on uniform 129×129 and 257×257 grids, respectively: all features of the secondary vortices are correctly predicted by the proposed primitive variable method.

5.3. The backward facing step. The second test problem is the determination of the separated flow in a sudden expansion inside a doubly infinite channel (backward facing step). The representative geometry for such a flow is shown in the figure together with a typical Delaunay mesh. The boundary conditions for such a problem include the Dirichlet velocity condition at the inlet $u_{|in} = (U(y), 0)$, where $U(y)$ is the Poiseuille profile $U(y) = -6(y - C)(y - S)/(C - S)^2$, C and S being the channel and step height, respectively, and homogeneous velocity conditions on the upper and lower solid walls and on the vertical side of the step. At the outlet the tangential velocity and the

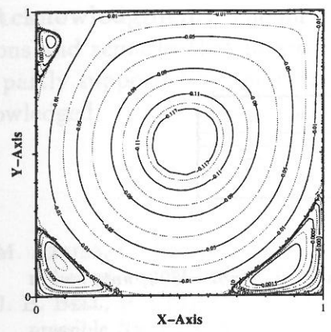

FIG. 9. *Streamlines for* $R = 3200$.

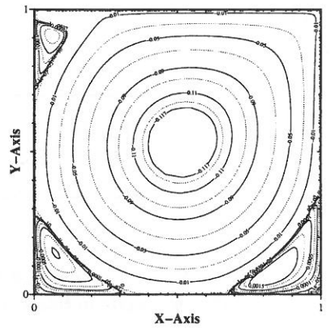

FIG. 10. *Streamlines for* $R = 5000$.

pressure are prescribed to be zero. The presence of a Dirichlet condition for pressure means that in the weak form of the momentum equation one has $v \cdot n_{|out} \neq 0$. The outlet boundary being defined by $x = constant$, the weak enforcement of $\nabla \cdot u = 0$ on it is accounted for only by the equation for the x component of velocity (in a strong setting the Neumann condition $(\partial u_x / \partial x)_{|out}$ would be imposed), whereas Dirichlet boundary conditions are imposed on the entire boundary on the y component. Therefore, the operators in the equations for the two velocity components are different and the two equations are uncoupled. As a consequence, the semi-implicit unconditionally stable scheme requires to build and factorize two different nonsymmetric sparse linear systems at each time step, but the two vector components of the intermediate velocity can be determined independently from each other.

The initial velocity $u_0(x, y)$ must be chosen so that it is compatible with the boundary values prescribed on velocity. The compatibility is guaranteed by "prolonging" the inlet Poiseuille velocity profile along the entire length of the channel, by taking

$$u_0(x, y) = \begin{cases} 0, & 0 \leq y \leq S \\ U(y), & S \leq y \leq C \end{cases}$$

The steady flow in a channel with $C = 1$ and $S = 1/2$ has been calculated for $R = 800$ using ≈ 4700 nodes and ≈ 8900 triangles distributed nonuniformly over a length $L = 20$. The streamlines of the solution displayed in figure 11 show two recirculatory regions, one on the lower wall with the reattachment point located at $x = 5.8/C$ downstream the step, and the other on the upper wall with separation and reattachment points located at $x = 6.1/C$ and $x = 9.0/C$ downstream the step. These values can be compared with the values 5.93, 4.78 and 10.21 obtained by a pressure correction finite difference method [22]. This discrepancy can be explained, at least partly, by the shorter section of the channel considered in the present calculation (*i.e.* difference in the boundary conditions) and the obvious lack of refinement of the mesh

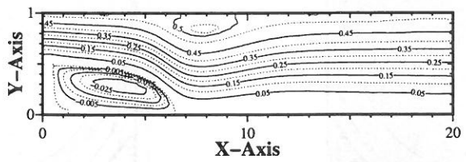

FIG. 11. *Backward facing step; streamlines for $R = 800$; note the two recirculating zones.*

that we used (systematic comparisons of refined solutions is out of the scope of the present paper).

6. Conclusions.

Fractional-step projection techniques are simple to implement, if implemented correctly: in practice we have to solve a succession of convection diffusion problems and Poisson problems. They are fast: the amount of computation is much lower than that required by coupled techniques such those which are based on the Uzawa operator. They yield first order accuracy in time in the natural norms; it is conjectured that second order should be achievable in some weaker norms as described in Rannacher [25]. In practice second order accuracy in time is observed though mesh dependent estimates can be proved [15]. If implemented correctly, the projection techniques are very robust—a very desirable feature for industrial applications.

One argument often raised against fractional-step projection techniques is that the homogeneous Neumann boundary condition imposed at the projection step is not "physical" and generally not satisfied by the "exact" solution. In the one hand, this point is correct in the sense that the Neumann boundary condition is responsible for a limitation of the accuracy order in time (possibly second order in some weak norms), but in the other hand this point is not completely relevant, for the projection techniques give convergence on the pressure only in the $L^2(\Omega)$ norm (hence inaccurate boundary values of pressure are theoretically admissible and should thus be of no concern). In short, users of projection techniques should recall that these techniques are meaningful only in the weak sense (they are based on a Hilbertian projection) and appropriate functional setting must accommodate two different spaces for representing the two velocity fields calculated in the viscous and incompressible half steps. Any attempt to formulate numerical approximations of projection techniques within strong frameworks (*i.e.* in some strong sense) is very likely to fail and will compell the authors of such attempts to claim that projection techniques suffer from "unphysical" boundary conditions. Of course, if for some reason one desires to achieve at each time step a convergence on the pressure in a much stronger norm than that of $L^2(\Omega)$, one certainly should not use projection techniques but should better try preconditioned Uzawa techniques.

Acknowledgment. The authors are grateful to Alfio Quarteroni for helpful discussions and remarks that improved the content of this paper. The present work has been partly supported by the Galileo Program; the support of this program is greatly acknowledged.

REFERENCES

[1] M. AZAIEZ, C. BERNARDI AND M. GRUNDMANN, Méthodes spectrales pour les équations du milieu poreux, **R 93029**, Laboratoire d'Analyse Numérique, Paris VI, 1993.

[2] J. B. BELL, P. COLELLA AND H. M. GLAZ, A second order projection method for the incompressible Navier–Stokes equations, *J. Comput. Phys.*, **85**, 1989, 257–283.

[3] H. BREZIS, *Analyse fonctionnelle, théorie et applications*, Masson, Paris, 1983.

[4] F. BREZZI, On the existence uniqueness and approximation of saddle-point problems arising from Lagrangian multipliers, *R.A.I.R.O.*, **R.2**, 1974, 129–151.

[5] O. R. BURGGRAF, Analytical and numerical studies of the structure of steady separated flows, *J. Fluid Mech.* **24**, 1966, 113–151.

[6] A. J. CHORIN, Numerical solution of the Navier–Stokes equations, *Math. Comp.*, **22**, 1968, 745–762.

[7] A. J. CHORIN, On the convergence of discrete approximations to the Navier–Stokes equations, *Math. Comp.*, **23**, 1969, 341–353.

[8] R. DAUTRAY AND J.-L. LIONS, *Analyse mathématique et calcul numérique pour les sciences et les techniques*, Masson, Paris, 1984

[9] J. DONEA, S. GIULIANI, H. LAVAL AND L. QUARTAPELLE, Finite element solution of the unsteady Navier–Stokes equations by a fractional step method, *Comput. Meths. Appl. Mech. Eng.* **30**, 1982, 53–73.

[10] J. A. GEORGE, An automatic one-way dissection algorithm for irregular finite element problems, *SIAM J. Numer. Anal.*, **17**, 1980, 740–751.

[11] J. A. GEORGE AND J. W.-H. LIU, *Computer Solution of Large Sparse Positive Definite Systems*, Prentice-Hall, Englewood Cliffs, N. J., 1981.

[12] U. GHIA, K. N. GHIA AND C. T. SHIN, High-Re solutions for incompressible flow using the Navier–Stokes equations and multigrid method, *J. Comput. Phys.*, **48**, 1982, 387–411.

[13] V. GIRAULT AND P.-A. RAVIART, *Finite Element Methods for Navier–Stokes Equations*, Springer Series in Computational Mathematics, **5**, Springer-Verlag, 1986.

[14] P. M. GRESHO AND S. T. CHAN, On the theory of semi-implicit projection methods for viscous incompressible flow and its implementation via finite element method that also introduces a nearly consistent mass matrix. Part I and Part II, *Int. J. Numer. Methods Fluids*, **11**, 1990, 587–620.

[15] J.-L. GUERMOND, Some error estimates for the approximation of the unsteady Navier–Stokes equations by means of projection methods, *Int. J. Numer. Methods Fluids*, submitted, and LIMSI report **93-30**.

[16] J.-L. GUERMOND, Sur l'approximation des équations de Navier–Stokes instationnaires par une méthode de projection, *C. R. Acad. Sc. Paris*, Série I, **319**, 1994, 887–892, and LIMSI report **94-03**.

[17] J.-L. GUERMOND, Perturbations singulières des problèmes de point selle et préconditionement du problème de Stokes, *Modél. Math. Anal. Numér.*, **28**, 1994, 357–374.

[18] J. G. HEYWOOD AND R. RANNACHER, Finite element approximation of the nonstationary Navier–Stokes problem, I, II, III, and IV, *SIAM J. Numer. Anal.*, **19**, 1982, 275–311, **23**, 1986, 750–777, **25**, 1988, 489–512, **27**, 1990, 353–384.

[19] H.-C. KU, R. S. HIRSH AND T. D. TAYLOR, A pseudospectral method for solution of the three-dimensional incompressible Navier–Stokes equations, *J. Comput. Phys.* **70**, 1987, 439–462.

[20] J.-L. LIONS, E. MAGENES, *Problèmes aux limites non homogènes et applications*, Dunod, Paris, 1968.

[21] A. N. F. MACK, An element level zero-divergence finite element approach, *Int. J. Numer. Meth. Fluids* **19**, 1994, 795–813.

[22] L. PENTARIS, K. NIKOLADOS AND S. TSANGARIS, Development of projection and artificial compressibility methodologies using the approximate factorization technique, *Int. J. Numer. Meth. Fluids* **19**, 1994, 1013–1038.

[23] L. QUARTAPELLE, *Numerical Solution of the Incompressible Navier–Stokes Equations*, ISNM **113**, Birkhäuser, Basel, 1993.

[24] A. QUARTERONI AND A. VALLI, *Numerical Approximation of Partial Differential Equations*, Springer Series in Computational Mathematics, **23** Springer-Verlag, 1994.

[25] R. RANNACHER, On Chorin's projection method for the incompressible Navier–Stokes equations, *Lectures Notes in Mathematics*, **1530**, Springer, Berlin, 1992, 167–183.

[26] S. REBAY, Efficient unstructured mesh generation by means of Delaunay triangulation and Bowyer–Watson algorithm, *J. Comput. Phys.*, **106**, 1993, 125–138.

[27] R. TEMAM, *Navier–Stokes Equations*, Studies in Mathematics and its Applications, 2, North-Holland, 1977.

[28] R. TEMAM, Une méthode d'approximation de la solution des équations de Navier–Stokes, *Bull. Soc. Math. France*, **98**, 1968, 115–152.